Magnesium Technology 2012
Edited by: Suveen N. Mathaudhu, Wim H. Sillekens, Neale R. Neelameggham, and Norbert Hort
TMS (The Minerals, Metals & Materials Society), 2012

EFFECT OF THE SOLIDIFICATION RATE ON MICROSTRUCTURE OF CAST Mg ALLOYS AT LOW SUPERHEAT

Gregory Poole[1], Nathan Rimkus[2], Aeriel Murphy[1], Paige Boehmcke[1], and Nagy El-Kaddah[1]
[1] Department of Metallurgical Engineering, University of Alabama, Tuscaloosa, Alabama 35487 USA
[2] Los Alamos National Laboratory, Los Alamos, New Mexico 87545 USA

Keywords: Mg alloys, Solidification Rate, Grain Structure, Microsegregation

Abstract

This paper investigates the effect of cooling rate on the grain size and microstructure of Mg AZ31B alloy cast at a superheat of 8°C using the Magnetic Suspension Melting (MSM) process, which is capable of melting and casting at superheats less than 5°C. In this study, the Mg alloy was unidirectionally solidified in a bottom-chill mold with stainless steel and copper chill blocks. The solidification parameters, namely growth velocity (V) and temperature gradient (G), were determined from numerical simulation of the cooling curves, which was found to be in good agreement with measurements. For the investigated solidification rates, metallographic examination showed globular solidification morphology, and the grain size was inversely proportional to the square root of the cooling rate. Microprobe analysis of the cast ingots also showed that Al segregation occurs primarily at the grain boundaries, and the solidification rate affects the size and distribution of both the secondary α phase and the intermetallic $Mg_{17}Al_{12}$ phase.

Introduction

In recent years, there has been considerable interest in casting magnesium automotive components as a mean to reduce the overall weight of the cars, thus improving fuel efficiency [1]. To produce quality products with a high degree of reliability, it is critical to minimize the effect of casting defects on mechanical properties of the cast alloy. One such defect is solute segregation in the as-cast alloy, which is known to be detrimental to mechanical properties [2-4]. For typical solidification rates for sand and die castings in the range of 0.1-100°C/s, the grain structure is dendritic, with segregation of the alloying elements in the matrix between the secondary dendrite arms,. Therefore, it is important to reduce the extent of solute segregation in the matrix by reducing the grain size, which generally depends on the solidification rate (V) [5].

Previous studies have shown that increasing the solidification rate reduces both the secondary dendrite arm spacing (SDAS) and the amount of secondary phases between the dendrite arms [6-8]. To achieve the desired mechanical properties of the cast Mg alloys, much effort has been focused on grain refinement via the addition of grain refiners as a means to reduce the SDAS at the same solidification rate [9-11]. This approach, however, does not completely eliminate solute segregation of the alloying elements in cast products.

It is well established that casting at low superheat not only reduces the grain size, but the solidification morphology of the casting from a dendritic to a globular structure, further preventing segregation within the grains. The idea of behind this technique is to suppress the growth of dendrite arms by reducing the temperature gradient (G) at the solidification front.

Previous studies on casting superalloys using the Microcast X technology have shown that a superheat of approximately 10°C produces fine grains around 100 μm [12-14]. Studies on melting and casting Al-Li and Mg alloys at such low superheat using the Magnetic Suspension Melting (MSM) process have shown that the castings are homogenous, oxide free, and exhibit a fine globular grain structure. The average grain size for Al-Li 2090 and 8090 alloys unidirectionally-solidified using a stainless steel bottom chill mold was about 30 μm [15,16], while that for Mg AZ31B alloy was approximately 80 μm [17,18]. These studies have also shown that segregation of secondary and intermetallic phases did not occur within the grain, but rather only at the grain boundaries. This paper examines the effect of solidification rate on the as-cast grain structure and micro/macro segregation of Mg AZ31B alloy at low superheat by varying the thermal properties of the chill block.

Experimental Technique

Casting of Mg AZ31B at low superheat was carried out using the MSM process, which is an integrated containerless induction melting and casting process specifically developed for reactive metals such as Mg. The experimental system is comprised of two main components: the melting compartment and the casting chamber as illustrated in Figure 1, thus combining melting and casting into a single, seamless operation, where the charge is melted in the melting compartment and pours into the mold located in the casting chamber. A detailed description of the experimental system used in this study is given in Reference [18].

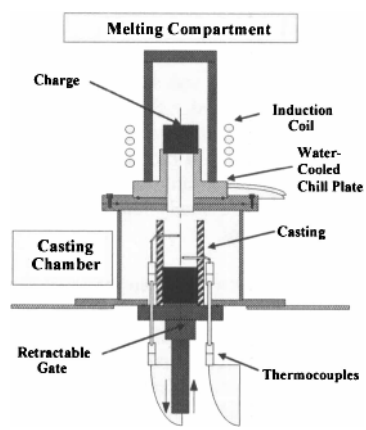

Fig 1. Schematic of the MSM system

All experiments were conducted using an Mg AZ31B alloy with composition Mg-3.143%Al-0.66%Zn-0.377%Mn-0.051%Si. A typical experimental run involved placing short bars 76 mm in diameter and 63 mm high into the melting compartment and flushing the system with argon at a rate of 8.5 L/min . The coil was then energized, adjusting the current as necessary to maintain a constant superheat of 8°C. Upon melting the charge, the metal was poured into a bottom-chilled mold shown in Figure 2. The ceramic mold was a 153 mm silica tube with 76 mm ID and 89 mm OD produced by Zircar Refractory Composites Inc. The stainless steel and copper chill blocks used in this study were 76 mm in diameter and 50 mm high. A battery of thermocouples was used to measure the cooling rates at different heights in the center of the mold, and was attached to an Omega TC-08 data acquisition system.

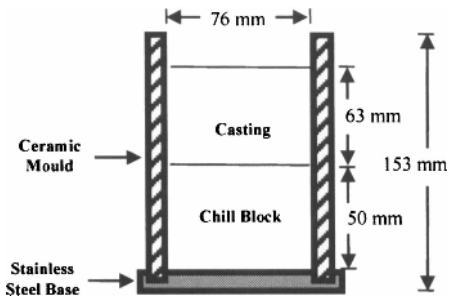

Fig 2. Sketch of the casting mold.

Characterization of the cast microstructures included optical microscopy and microprobe analysis. Optical micrographs were taken using a Nikon Epiphot 200 optical microscope, and EDS mapping of solute distribution was done using a JEOL 8600 FE SEM EPMA. The solidification parameters V and G were determined from numerical simulation of the cooling curves.

Results and Discussion

In the following, we shall present the results of the thermal analysis of the cooling curves used in the determination of the solidification parameters for MSM cast Mg AZ31B alloy on copper and stainless steel chill blocks at superheat of 8°C, together with the observed grain structure and segregation of Al for these two cases.

Figure 3 shows the computed and measured cooling curves of the cast alloy in the mold for copper and stainless steel chill plates. The lines indicate the computed values while the symbols correspond to experimental measurements. This figure shows that the cooling rate for the copper chill block is about twice that of the stainless steel chill block, as would be expected. It also shows that the solidification model accurately reproduces the measured cooling curves within ±5 percent.

Figure 4 shows an expanded view of the cooling curves within the solidification range. As seen in this figure, the experimental solidification times for copper and stainless steel chill blocks were found to be 24.7s and 36.1s, respectively. Although the model accurately predicts these total solidification times, it reasonably predicts the temperature evolution in the mushy region. This is mainly due to the difference between the actual and modeled evolution of latent heat during solidification.

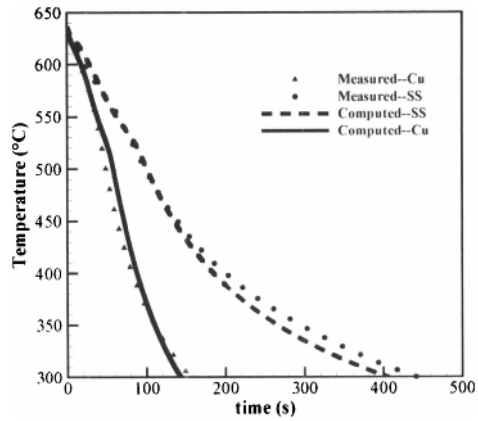

Fig 3. Measured and computed cooling curves for cast Mg AZ31B alloy over copper and stainless steel chill blocks.

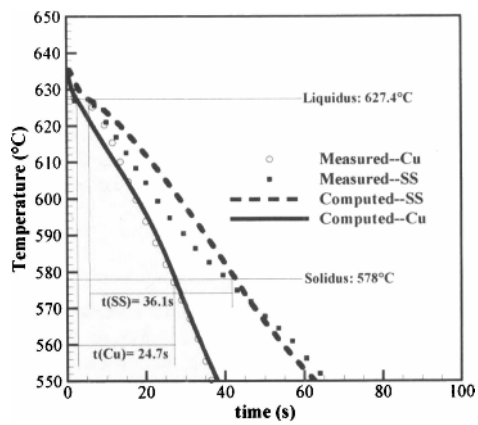

Fig 4. Cooling curves for solidification region.

From these two curves, solidification parameters G and V were evaluated. Figure 5a shows the rate of advance of the solidified layer. As seen in this figure, the growth velocity V is almost constant over the entire height of the casting for both copper and stainless steel chill blocks. The mean growth velocities for the Mg casting on copper and stainless steel chill blocks were 0.75 mm/s and 0.6 mm/s, respectively. In contrast, the value of G at the solidification front depend on the height of the casting, Figure 5b, and is mainly due to the increase of thermal resistance of heat extraction in the chill block during solidification. For solidification on copper chill block, G decreases from 3.5 °C/mm at the bottom of the mold to 2.5 °C/mm at the top of the ingot, with an average value of 3 °C/mm. The corresponding G values for the stainless steel chill block ranged from 3.5 °C/mm to 1.5 °C/mm, with an average value of 2.5 °C/mm. From these values, the average cooling rate, which is used to correlate the grain size with solidification rate [7], was evaluated. For copper chill block, the cooling rate is 2.25 °C/s, while for stainless steel the value was 1.5 °C/s. It is important to note that for castings at high superheats these solidification parameters correspond to equiaxed dendritic solidification morphology [5].

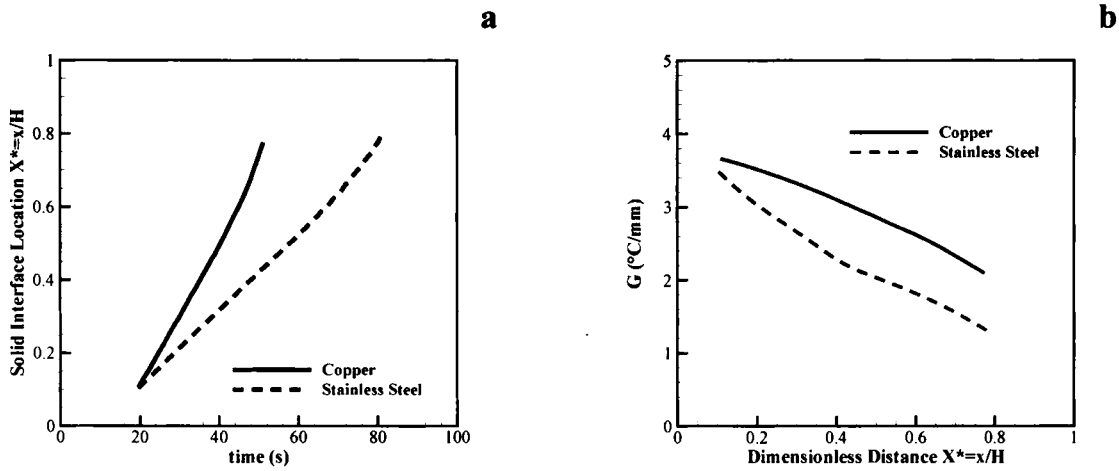

Fig 5. Solidification parameters for copper and stainless steel chill blocks: (a) solidification rate V , (b) Temperature gradient G.

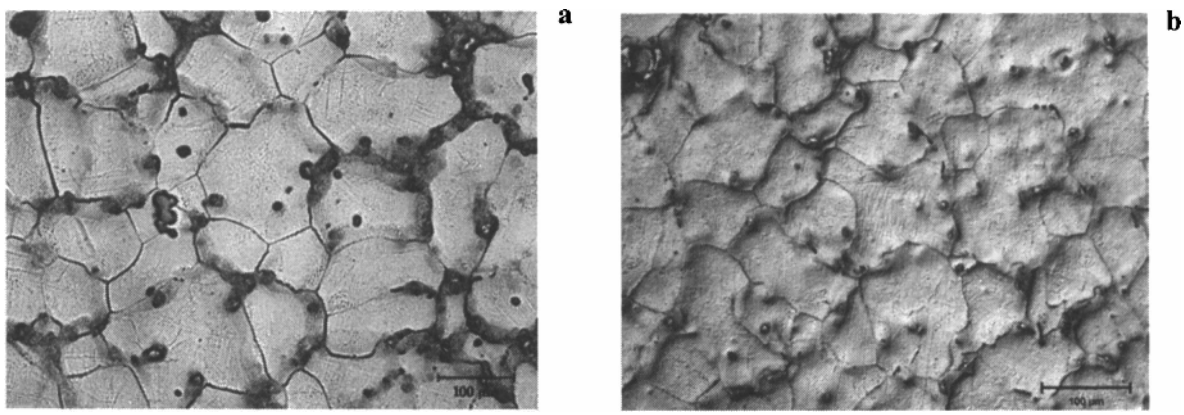

Fig 6. Grain structure of MSM cast Mg AZ31B at 8°C superheat at 200 X for: (a) stainless steel and (b) copper chill blocks

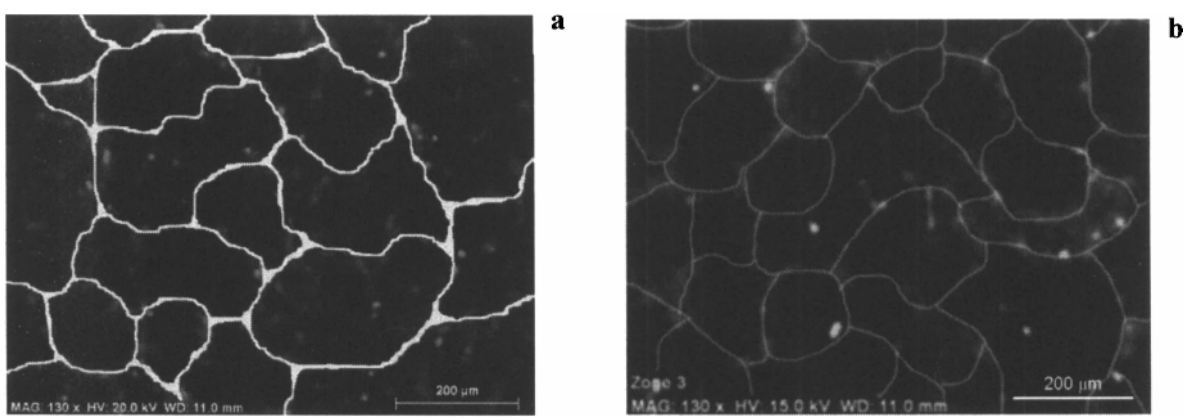

Fig 7. EDS Maps of Al solute distribution in MSM cast Mg AZ31B at 8°C superheat for: (a) stainless steel and (b) copper chill blocks

Figures 6a and 6b show the optical micrographs of the grain structures for cast Mg AZ31B on copper and stainless steel chill blocks at a superheat of 8°C. In these micrographs the brighter areas are the α-Mg phase, while the darker areas at the grain boundaries correspond to the Al-rich secondary-α phase and $Mg_{17}Al_{12}$ intermetallics. This suggests globular solidification morphology for cast Mg alloys at low superheat [17,18]. Further inspection shows that the average grain size for a solidification rate of 0.6 mm/s, which corresponds to stainless steel chill block, is 92 μm, while that of the copper chill block solidification rate of 0.75 mm/s is approximately 75 μm. These results suggest that the grain size is inversely proportional to the square root of the cooling rate. Work is currently in progress to obtain more data to develop a more accurate correlation between the grain size and the cooling rate.

Figure 7 shows the EDS maps of Al segregation for the two cases investigated. The light areas correspond to Al-rich secondary-α phase, while the more bright spots are the $Mg_{17}Al_{12}$ intermetallic. These phases are essentially found at the grain boundaries, which further confirm globular solidification morphology. It is also seen that the solidification rate affects the size and distribution of these phases. Moreover, the observed minor entrapment of secondary-α and $Mg_{17}Al_{12}$ phases in the matrix suggest that the superheat of 8°C corresponds to the transition temperature from a globular to dendritic structure.

Conclusions

The effect of the rate of cooling on the microstructure of cast Mg AZ31B alloy at low superheat of 8°C was investigated experimentally and theoretically. The experimental study was carried out using the MSM process, which is capable of melting and casting metals at very low superheat. Casting experiments were carried out in a bottom chill copper and stainless steel molds. The solidification rates V and temperate gradients G for these two chill blocks were determined from a heat transfer model of the solidification process, which accurately predicts the experimentally measured cooling curves for these two chill blocks. All castings exhibited fine-grained globular structure with grain size less than 100 μm, and the grain size was found to inversely proportional to the square root of the cooling rate. Microprobe analysis of Al segregation showed that the secondary-α and $Mg_{17}Al_{12}$ phases are mostly segregated at the grain boundaries, thus confirming that casting at low superheat promote the transition from dendritic to globular solidification morphology for Mg alloys.

Acknowledgements

The authors graciously thank the NSF for funding this project under grant number CMMI-0856320. Also, we would like to thank Rob Holler of the Central Analytical Facility at the University of Alabama for his help in using the Microprobe.

References

1. "Magnesium Vision 2020: A North American Automotive Strategic Vision for Magnesium," Automotive Metals Division, United State Automotive Materials Partnership (USAMP) (November 2006).

2. S.G. Lee, et al., "Characterization of the effects of process parameters on macrosegregation in a high-pressure die cast magnesium alloy," *Materials Characterization*, 55 (2005), 219-224.

3. D.G.L. Prakash and D. Regener, "Quantitative characterization of Mg17Al12 phase and grain size in HPDC AZ91 magnesium alloy," *Journal of Alloys and Compounds*, 2007, 461, 139-146.

4. S.I. Bakhtiyarov and R.A. Overfelt, "First V-Process casting of magnesium," *Proceedings of Magnesium Technology 2004*, ed. A.A. Luo, (Warrendale, PA: TMS, 2004), 187-192.

5. K. Fisher, *Fundamentals of Solidification* (Aedermannsdorf, Switzerland: Trans Tech Publications, 1986), 88.

6. D.H. Kang, M. Paliwal, E. Essadiqi, and I.H.Jung, "Experimental Studies on the As-Cast Microstructure of Mg-Al Binary Alloys with Various Solidification Rates and Compositions," *Proceedings of Magnesium Technology 2010*, eds. S.R. Agnew et al, (Warrendale, PA: TMS, 2010), 533-536.

7. M. Masoumi and M. Pekguleryuz, "Effect of Cooling Rate on the Microstructure of AZ31 Magnesium Alloy," *AFS Transactions*, 2009, 617-626.

8. Y. He, A. Javaid, E. Essadiqi, and M. Shehata, "Numerical Simulation and Experimental Study of the Solidification of a Wedge-Shaped AZ31 Mg Alloy Casting," *Canadian Metallurgical Quarterly*, 48 (2) (2009), 145-156.

9. Q. Jin, J.P. Eom, S.G. Lim, W.W. Park and B.S. You, "Grain Refining Mechanism of a Carbon Addition Method in a Mg-Al Magnesium Alloy," *Scripta Materialia* 49(2003), 1129-1132.

10. G. Han, X. Liu, and H. Ding, "Grain Refinement of AZ31 Magnesium Alloy by New Al-Ti-C Master Alloys," *Transactions of Nonferrous Metals Society of China*, 19(2009), 1057-1064.

11. P. Cao, M. Quian, and D.H. St. John, "Native Grain Refinement of Magnesium Alloys," *Scripta Materialia*, 53(2005), 841-844.

12. Brinegar, J.R., *et al.*, U.S. patent, No. 4832112 (1989).

13. Y. Ma, et al., *Journal of Materials Processing Technology*, 137(2003), 35-39.

14. L. Liu, et al., *Materials Science and Engineering A* 394(2005), 1-8.

15. D. J. Reynolds, M. Shamsuzzoha, and N. El-Kaddah, "Characterization of Al-Li Castings Produced by the Magnetic Suspension Melting Process," *Proceedings of the 4th Decennial International Conference on Solidification Processing*, eds. J. Beech and H. Jones, (Sheffield, UK: University of Sheffield, 1997), 45-48.

16. C. Mahato, M. Shamsuzzoha, and N. El-Kaddah, "Solidification Morphology and Structure of Cast Al-Li 2090 Alloy at Low Superheats," *Solidification of Aluminum Alloys*, eds. M.G. Chu et al., (Warrendale, PA: TMS, 2004), 321-328.

17. N. Rimkus, L. Vihtelic, and N. El-Kaddah, "Grain and Microstructure of Cast Mg. AZ31B Alloy Produced by the Magnetic Suspension Melting Process," *Proceedings of Light Weight Materials for Vehicles and Components Symposium*, (Warrendale, PA: TMS, 2004), 753-761.

18. N.W. Rimkus, M.L. Weaver, and N. El-Kaddah, "Microstructure and Mechanical Behavior of Cast Mg AZ31B Alloy Produced by the Magnetic Suspension Melting Process," *Proceedings of Magnesium Technology 2011*, eds. W. Silleken et al., (Warrendale, PA: TMS, 2011), 335-343.